Roughness of Two-Dimensional Cracks in Wood

Thor Engøy and Knut Jørgen Måløy
Fysisk Institutt, Universitetet i Oslo, Postboks 1048 Blindern, N-0316 Oslo, Norway

Alex Hansen*
Groupe Matière Condensée et Matériaux, URA CNRS 804, Université de Rennes I, Campus de Beaulieu F-35042 Rennes Cedex, France

Stéphane Roux
Laboratoire de Physique et Mécanique de la Matière Hétérogène, URA CNRS 857, Ecole Supérieure de Physique et Chimie Industrielles de Paris, 10 rue Vauquelin, F-75231 Paris Cedex 05, France
(Received 3 August 1993)

Fractures in wood that are parallel to the fibers will be quasi-two-dimensional in the orthogonal directions. We have measured the roughness of fractures in Malaysian nemesu and Norwegian spruce wood. Tangential and radial fracture surfaces have very different morphologies due to the strong anisotropy of wood, but the scaling properties seem to be the same. We determine the roughness exponent ζ to be 0.68 ± 0.04, where the average is taken over different woods, fracture modes, and analyses. These results support the conjecture of a universal roughness exponent of brittle fracture surfaces.

PACS numbers: 61.43.Hv, 07.60.−j, 62.20.Mk

Since the seminal work of Mandelbrot, Passoja, and Paullay [1] there has been a simmering interest in the geometrical properties of fracture surfaces. There is now ample evidence [2] that fracture surfaces possess statistically self-affine scaling properties [3].

A self-affine surface, $z(x,y)$, isotropic in the (x,y) plane, is invariant under the scale transformation

$$(x,y,z) \rightarrow (\lambda x, \lambda y, \lambda^{\zeta} z), \quad (1)$$

where ζ is the *roughness exponent.* The values of ζ reported in the literature all seem to be in the range 0.7 to 0.9 [4–11] for measurements with a resolution down to the micron scale. A careful study by Bouchaud, Lapasset, and Planès [7] of a slightly ductile aluminum alloy having undergone a range of different heat treatments resulted in a roughness exponent $\zeta = 0.80 \pm 0.05$ independent of the heat treatment. This led the authors to propose that the roughness exponent could be *universal* (independent of the material for a range of materials). This study was followed by that of Måløy *et al.* [8] using six very different brittle materials. As in the Bouchaud study, scaling was found over 2 orders of magnitude in length scales, and the roughness exponent of all materials involved turned out to be $\zeta = 0.87$ with a precision of about 10%, consistent with the hypothesis of a universal roughness exponent. The universality hypothesis has been contested by Milman *et al.* who studied fractures on the nanometer scale [12] (about 3 orders of magnitude smaller than in the studies of Refs. [4–11]). These authors found a roughness exponent that strongly depends on the material. Other studies covering the same range of length scales found the same wide range of exponents [13]. It thus seems that, if there is a universality class for brittle fracture roughness, these extremely small length scales are outside its range of validity.

These measurements have all been done on *three-dimensional* materials. Hansen, Hinrichson, and Roux [14] studied the roughness of fractures in the *two-dimensional* fuse model [15] with a range of very different disorders and found the same roughness exponent $\zeta = 0.7$ with a precision of about 10%. An experimental study of breakdown in two-dimensional packings of collapsible cylinders gave a result consistent with this exponent [16]. However, the precision with which the roughness exponent could be determined in this experiment was fairly low. In addition, the mechanical behavior was not elastic brittle. A careful study of rupture lines in Ref. [17] gave a roughness exponent of 0.68 ± 0.04. Here the problem of out of plane deformations was not discussed, although it is crucial in deciding the dimensionality of the system. As paper cannot support a compressive stress, even without buckling, the stress field is confined to a very narrow zone at the crack tip. This contrasts with an elastic medium where the crack field is long ranged.

The experimental works cited above are all on isotropic materials with the possible exception of paper. Many natural and designed materials have anisotropic mechanical properties, e.g., due to structural reinforcements in a preferred direction (notable examples are wood and reinforced concrete). It is important in applications such as construction to understand how fractures in these materials are affected by the underlying morphology.

We report here a study of brittle fracture roughness in a two-dimensional system where the elastic properties are well established. We take care to probe the effect of anisotropy of the material on the scaling of the

0031-9007/94/73(6)/834(4)$06.00

fracture surfaces. Thus we are able to test the universality conjecture in two dimensions for an anisotropic elastic brittle material.

Wood was chosen because of its structural anisotropy and because fractures generated between fibers give rise to quasi-two-dimensional surfaces; i.e., they are almost invariant in the axial direction. The presence of radially running ray cells is the main qualitative feature giving the anisotropy in the radial and tangential directions.

Seasonal variations cause a heterogeneous density in wood. To ensure a relatively large amplitude in the roughness of the fracture surfaces we selected specimens having large growth rings from two commercially available wood species, Malaysian nemesu (*Shorea Pauciflora*) and Norwegian spruce (*Picea Abies*). The nemesu specimens had a density (ρ) of 540 kg/m^3 (dry weight/dry volume), a moisture content (u) of 3.0% (moisture weight/dry weight), and growth rings approximately 3 cm wide. However, minor variations on a scale of 4 mm were also visible. Typical values for the spruce specimens were $\rho = 330$ kg/m^3, $u = 5.4\%$, and growth rings were about 5 mm wide.

The samples were prepared by sawing cross sections, of various lengths in the axial direction, from 2 in. planks. Two methods of breaking were employed: bending and stretching. Before bending, the samples were clamped between a metal plate and a table. Fracture was generated along an average tangential or radial direction by aligning the growth ring tangent along or perpendicular to the sample holder. Stretching was performed in a laboratory tensile testing machine. A small notch was cut to control crack initiation.

Evidently size, orientation, and linkage of structural elements in wood are important in determining the validity of a scaling assumption. Under loading the cell wall breaks, revealing structure even below cell size. However, a coarse graining at a larger length scale is due to the orthogonal connection between tracheids and vessels running axially and ray cells running radially. This anisotropy makes the fracture surface deviate from a quasi-two-dimensional surface.

Most tracheid cells in the nemesu samples were about 25 μm in diameter. Vessel elements were about an order of magnitude larger. Rays interspersed groups of tracheids 8–12 cells wide. This led us to introduce a typical lower cutoff in the data around 250 μm. Cleavage along the rays was also important in flattening the radial fracture surfaces. Amplitudes in the radial cracks were up to 1 mm, while the tangential cracks had peaks up to 3 mm. The difference in morphology between tangential and radial fracture is clearly seen from the two profiles in Fig. 1. Curvature of the growth rings was apparent in the spruce samples which were broken 10–15 cm from the pitch. In Table I we list details of the various samples studied.

We recorded the surfaces with a needle-arm profilometer [8]. The samples, mounted on a translation stage, were moved past the needle under step motor control. As the needle moved up or down, a mirror on the axis of the arm rotated. The position of a reflected laser beam was measured with a photodiode giving a voltage signal proportional to the height of the surface. Thus a trace $z = z(x)$ was recorded. Surface profiles over a length of 2.56 cm were measured using a step length of 12.5 μm for test set E (see Table I) and 25 μm for all the other samples. The setup was calibrated for a maximum peak of 4 mm. Vertical resolution, estimated from the difference between two successive scans along the same line, was about 5 μm.

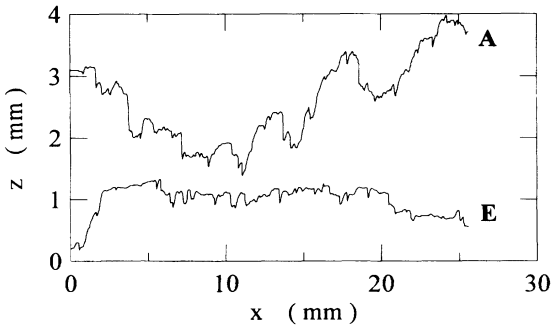

FIG. 1. Surface profiles of nemesu samples. The top curve shows a tangential fracture surface from data set A. Below is a radial fracture from set E.

Analysis of the data was performed using three very different methods: the first return probability method [8], the power spectrum [3], and the bridge method [18]. We subtracted off the drift in each trace by transforming $z(x) \rightarrow z(x) - [z(x_{\max}) - z(x_{\min})] \times (x - x_{\min})/(x_{\max} - x_{\min})$, where $x_{\min} \leq x \leq x_{\max}$.

TABLE I. List of fracture samples analyzed. The samples are classified by surface (tangential or radial), mode of fracture (*S* for stretching or *B* for bending), and sample thickness. Unless otherwise stated the samples are all nemesu wood. Roughness exponents are calculated for each test set using the first return probability, the power spectrum, and the bridge method.

Fracture test	Sample No.	d (mm)	First return	Power spectrum	Bridge
A Tan. *S*	7	6.1	0.67	0.63	0.63
B Rad. *S*	8	6.1	0.71	0.47	0.68
C Tan. *B*	5	6.5	0.60	0.67	0.72
D Rad. *B*	5	6.5	0.68	0.60	0.74
E Rad. *B*	5	6.5	0.74	0.69	0.69
F Tan. *B*	4	4.3	0.64	0.69	0.70
G Tan. *B*	4	7.7	0.67	0.70	0.70
H[a] Tan. *B*	9	7.7	0.62	0.70	0.69
$\langle\zeta\rangle$[b]			0.67	0.67	0.69
σ_ζ			0.05	0.04	0.03

[a]Spruce.
[b]Average roughness exponent.

The *first return probability method* consists in measuring the probability that a height z appearing at position x reappears for the first time at distance $x + \Delta$. This probability distribution $R(\Delta)$ follows a power law in Δ,

$$R(\Delta) \sim \Delta^{-(2-\zeta)}/(L - \Delta). \quad (2)$$

We have here introduced the finite size correction $1/(L - \Delta)$ which takes into account that any return distance Δ must lie within the interval $[0, L]$.

Figure 2 shows the first return probability distributions for test sets A, B, and C. Excluding the region below 0.125 mm and the noise above 1.5 mm, we have made linear least-squares fits guided by eye. The lower cutoff is of the same order as determined earlier on physical grounds. The roughness exponents found with this method are listed in Table I and the average is $\zeta = 0.67 \pm 0.05$. All of the uncertainties reported in this paper are statistical standard deviations. Without the correction factor we obtain an average value which is about 4% lower.

The second method used is to calculate the *power spectrum,* that is, the Fourier transform of the correlation function $\langle z(x + \Delta x)z(x)\rangle$. The power spectrum scales as

$$P(f) \sim f^{-(1+2\zeta)}. \quad (3)$$

Figure 3 shows the averaged power spectrum for test sets A, B, and C. The linear least-squares fits were generally made between $\log_{10} f = -1.4$ and 1 (1/mm), the latter corresponding to about half the physical cutoff length. However, the spectrum for B is more curved than the others; see Fig. 3. Here we fitted the range between $\log_{10} f = -1$ and 0.6. Most samples in set B were very flat and this may have reduced the power in the low frequency part significantly. In Table I we give the roughness exponents determined from power spectra.

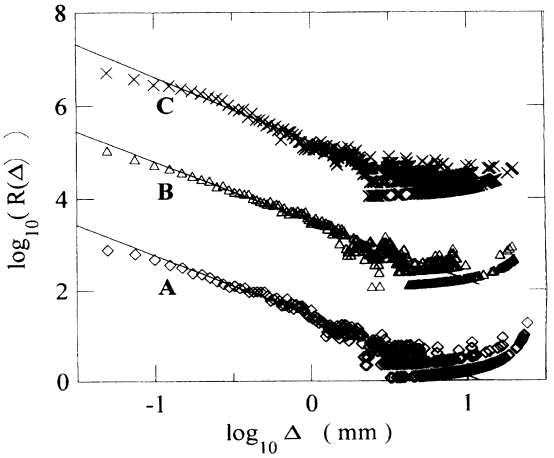

FIG. 2. First return probability distributions $R(\Delta)$ for tests A, B, and C. For clarity of presentation the data for B and C have been shifted upward 2 and 4 units (on log scale), respectively.

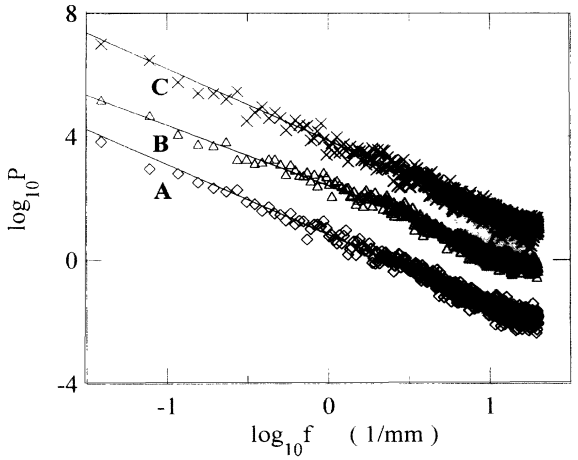

FIG. 3. Averaged power spectra, $P(f)$ for tests A, B, and C. The data for B and C have been shifted upward 2 and 3 units, respectively.

Leaving out the exceptionally low value for B, we get an average $\zeta = 0.67 \pm 0.04$.

The *bridge method* [18] consists in cutting the fracture trace into equal pieces of length X. The drift is subtracted from each piece, and then the distance between the maximum z and minimum z, $\Delta_{\max} z$, is recorded for pieces of different lengths X. We then average over all pieces of the same length. $\Delta_{\max} z$ scales as

$$\Delta_{\max} z \sim X^{\zeta}. \quad (4)$$

A plot of this law for data sets A, B, and C is shown in Fig. 4. The linear fits were made above the lower cutoff length. Averaging the roughness exponents obtained with this method gives $\zeta = 0.69 \pm 0.03$.

Since large corrections to scaling seem to be unavoidable, we felt it important to measure the roughness exponent with very different methods. This counteracts, at least partly, human bias in the analysis. The various methods are sensitive to different properties of the data. Both the first return method and the bridge method gave exponents in good agreement for set B indicating that the exceptional value from the power spectrum was a weakness of this method. The average values from all the methods are very close. As an estimate for the roughness exponent we therefore average over the various methods of analysis, woods, and fracture modes, except the power spectrum for B, to find $\zeta = 0.68 \pm 0.04$.

The absence of large fluctuations in Table I from this value supports the notion of a universal roughness exponent. Changing the thickness of a sample will change the amplitude, but not the scaling exponent. Again, that rather disparate morphologies as the radial and tangential fractures, see Fig. 1, seem to have the same scaling properties supports this hypothesis.

We have seen that a two-dimensional elastic brittle material, viz. wood, has a fracture roughness exponent

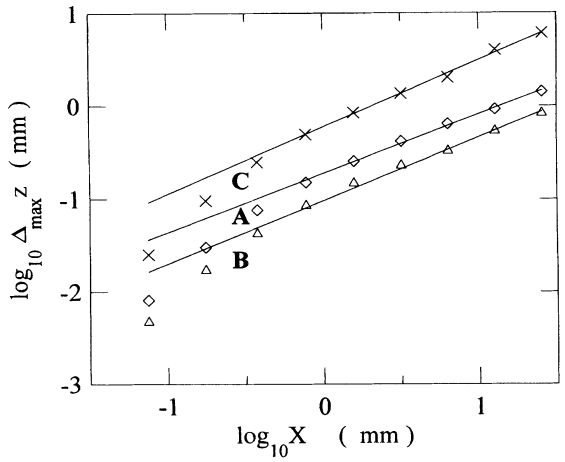

FIG. 4. Determination of the roughness exponent ζ from the bridge method for data sets A, B, and C. The data for B have been shifted 0.5 unit upward.

which is not sensitive to material species, fracture mode, or anisotropy. Consistency with previously mentioned studies [16,17] indicates that the simple two-dimensional elastic-brittle fracture process that is partly involved in these experiments controls the response of the systems. Additional nonlinearity (buckling, friction, etc.) play a minor role, which was not obvious initially.

It seems reasonable to assume that material properties should affect both the morphology and scaling of fracture surfaces. However, no clear understanding of what limits the class of materials having the same fracture roughness exponent has been reached. Attempts to correlate ζ with mechanical properties, e.g., toughness, of the materials investigated have not been conclusive (see Refs. [2,12] and [19]).

We have not systematically varied toughness. But, the two woods examined probe almost a factor of 2 in density, the most significant parameter characterizing the mechanical properties of wood. Therefore, a variation in toughness was tested indirectly without any measurable change in roughness exponent being detected. The same argument holds for earlier studies of a broad range of brittle and weakly ductile materials: By varying material, toughness was also varied.

A remaining issue is to identify the bounds of the class of systems having the same roughness exponent and the correct way to parametrize it.

This work was in part supported by GdR PMHC and GRECO Géomatériaux. We thank B. B. Mandelbrot for an enlightening discussion.

*Also at Institutt for Fysikk, NTH, N-7034 Trondheim, Norway.

[1] B. B. Mandelbrot, D. E. Passoja, and A. J. Paullay, Nature (London) **308**, 721–722 (1984).

[2] See, e.g., F. Tzschichholz and M. Pfuff, in *Fracture Processes in Concrete, Rock and Ceramics*, edited by J. G. M. van Mier, J. G. Rots, and A. Bakker (Cambridge Univ. Press, Cambridge, 1991), Vol. 1, or E. Bouchaud, in *Proceedings of the Conference Dislocations 92* (unpublished) for a review.

[3] B. B. Mandelbrot, *Fractals: Form, Chance, and Dimension* (Freeman, San Francisco, 1977); J. Feder, *Fractals* (Plenum, New York, 1989).

[4] S. R. Brown and C. H. Scholz, J. Geophys. Res. **90**, 12 575–12 582 (1985).

[5] Z. Q. Mu and C. W. Lung, J. Phys. D **21**, 848 (1988).

[6] J. J. Mecholsky, D. E. Passoja, and K. Feinberg-Ringel, J. Am. Ceram. Soc. **72**, 60 (1989).

[7] E. Bouchaud, G. Lapasset, and J. Planès, Europhys. Lett. **13**, 73–79 (1990).

[8] K. J. Måløy, A. Hansen, E. L. Hinrichsen, and S. Roux, Phys. Rev. Lett. **68**, 213–215 (1992); A. Hansen, T. Engøy, and K. J. Måløy, "Measuring Hurst Exponents with the First Return Method" (to be published).

[9] M. Tanaka, J. Mat. Sci. **27**, 4717 (1992).

[10] M. A. Issa, A. M. Hammad, and A. Chudnovsky, in *Engineering Mechanics*, edited by L. D. Lutes and J. M. Niedzwecki (American Society of Civil Engineers, New York, 1992).

[11] J. Schmittbuhl, S. Sentier, and S. Roux, Geophys. Res. Lett. **20**, 639 (1993).

[12] V. Yu. Milman, R. Blumenfeld, N. A. Stelmanshenko, and R. Ball, Phys. Rev. Lett. **71**, 204 (1993).

[13] L. A. Bursill, Fan XuDong, and Peng JuLin, Philos. Mag. A **64**, 443–464 (1991).

[14] A. Hansen, E. L. Hinrichsen, and S. Roux, Phys. Rev. Lett. **66**, 2476–2479 (1991).

[15] L. de Arcangelis, S. Redner, and H. J. Herrmann, J. Phys. (Paris), Lett. **46**, L585 (1985).

[16] C. Poirier, M. Ammi, D. Bideau, and J.-P. Troadec, Phys. Rev. Lett. **68**, 216–219 (1992).

[17] J. Kertész, V. Horváth, and F. Weber, Fractals **1**, 67–74 (1993).

[18] B. B. Mandelbrot (private communication).

[19] R. H. Dauskardt, F. Haubensak, and R. O. Ritchie, Acta Metall. Mater. **38**, 143–159 (1990).